JBC ARTICLE

PGAP6, a GPI-specific phospholipase A2, has narrow substrate specificity against GPI-anchored proteins

Received for publication, June 2, 2020, and in revised form, July 14, 2020 Published, Papers in Press, August 18, 2020, DOI 10.1074/jbc.RA120.014643

Gun-Hee Lee[1], Morihisa Fujita[2], Hideki Nakanishi[2], Haruhiko Miyata[1], Masahito Ikawa[1,3], Yusuke Maeda[1], Yoshiko Murakami[1,3], and Taroh Kinoshita[1,3,*]

From the [1]Research Institute for Microbial Diseases and the [3]Immunology Frontier Research Center, Osaka University, Osaka, Japan, and the [2]Key Laboratory of Carbohydrate Chemistry and Biotechnology, Ministry of Education, School of Biotechnology, Jiangnan University, Wuxi, Jiangsu, China

Edited by Dennis R. Voelker

PGAP6, also known as TMEM8A, is a phospholipase A2 with specificity to glycosylphosphatidylinositol (GPI) and expressed on the surface of various cells. CRIPTO, a GPI-anchored co-receptor for a morphogenic factor Nodal, is a sensitive substrate of PGAP6. PGAP6-mediated shedding of CRIPTO plays a critical role in an early stage of embryogenesis. In contrast, CRYPTIC, a close family member of CRIPTO, is resistant to PGAP6. In this report, chimeras between CRIPTO and CRYPTIC and truncate mutants of PGAP6 were used to demonstrate that the Cripto-1/FRL1/Cryptic domain of CRIPTO is recognized by an N-terminal domain of PGAP6 for processing. We also report that among 56 human GPI-anchored proteins tested, only glypican 3, prostasin, SPACA4, and contactin-1, in addition to CRIPTO, are sensitive to PGAP6, indicating that PGAP6 has a narrow specificity toward various GPI-anchored proteins.

Glycosylphosphatidylinositol (GPI)–anchored proteins (GPI-APs) are tethered to the outer leaflet of plasma membrane by a covalently linked glycolipid (1). Some GPI-APs are released from the cell surface after cleavage of the GPI anchor by GPI-specific hydrolytic enzymes (GPIases). There are several combinations of a select GPI-AP and a cognate GPIase with particular biological significance, such as testis-specific angiotensin-converting enzyme (tACE) cleaving the GPI anchors of TEX101 and LY6K in sperm (2, 3) by its putative endomannosidase activity (4). Shedding of these GPI-APs from sperm is critical for sperm maturation (3). Several members of the glycerophosphodiesterase (GDE) family are GPI-specific phospholipase C or D (PLC or PLD). GDE2 is involved in the shedding of RECK (reversion-inducing cysteine-rich protein with Kazal motifs), a GPI-anchored protease inhibitor, from certain neuronal cells, and the process is critical for neuronal differentiation (5). GDE2 is also involved in neuroblastoma differentiation through release of glypican 6 (GPC6) (6). GDE3 regulates cell adhesion, migration, and invasion by shedding uPAR, a GPI-anchored urokinase plasminogen activator receptor (7). GDE3 releases another GPI-AP, CNTFRα, from oligodendrocyte precursors and regulates their proliferation (8).

* For correspondence: Taroh Kinoshita, tkinoshi@biken.osaka-u.ac.jp.
Present address for Gun-Hee Lee: Korea Zoonosis Research Institute, Jeonbuk National University, Iksan, Jeonbuk, South Korea.

PGAP6, also known as TMEM8A, is a cell-surface phospholipase A_2 (PLA2) with specificity toward GPI (9) and is widely expressed (RRID:SCR_006710) (10). PGAP6 has a large extracellular portion in the N-terminal part and seven transmembrane (TM) domains in the C-terminal part. PGAP6 belongs to a superfamily, termed CREST for alkaline ceramidase, PAQR receptor, Per1, SID-1, and TMEM8 (11). The CREST superfamily includes several lipases that have conserved, presumably catalytic amino acids within the TM domains. We reported that CRIPTO, a GPI-AP (12), is a sensitive substrate of PGAP6 (9). CRIPTO plays a role in early embryonic development by acting as a co-receptor for a morphogenic factor Nodal (13, 14). PGAP6-dependent shedding of CRIPTO is critical for its role (9), especially for the generation of the anterior–posterior axis (15).

Mechanistically, PGAP6 acts on CRIPTO in the plasma membrane and removes one fatty acyl-chain from the GPI anchor, generating CRIPTO bearing only one fatty acyl-chain. CRIPTO that is anchored to the plasma membrane by a single fatty acyl-chain is released from the membrane either spontaneously or after removal of the lipid portion by a PLD, such as GPI-specific PLD (9).

CRYPTIC is another GPI-anchored, co-receptor for Nodal that also plays a role in early embryonic development, specifically in the generation of the left–right axis (16). CRIPTO and CRYPTIC are similar but expressed in different regions of the embryo and basically play independent roles (16). CRIPTO and CRYPTIC share 30% amino acid identity, have a similar domain organization, and belong to the same protein family, termed the EGF–Cripto-1/FRL1/Cryptic (CFC) family (17). In contrast to CRIPTO, CRYPTIC is resistant to PGAP6 (9). This indicates that PGAP6 differentiates the protein part of CRIPTO from that of CRYPTIC and selectively attacks the GPI anchor of CRIPTO but not CRYPTIC.

In this study, we aimed to understand the basis of the protein-selective action of PGAP6. We also aimed to determine whether CRIPTO is the only substrate of PGAP6 among more than 150 human GPI-APs.

Results

CFC domain of CRIPTO determines sensitivity to PGAP6

Both CRIPTO and CRYPTIC consist of an N-terminal signal sequence for translocation into the ER, an N-terminal (N)

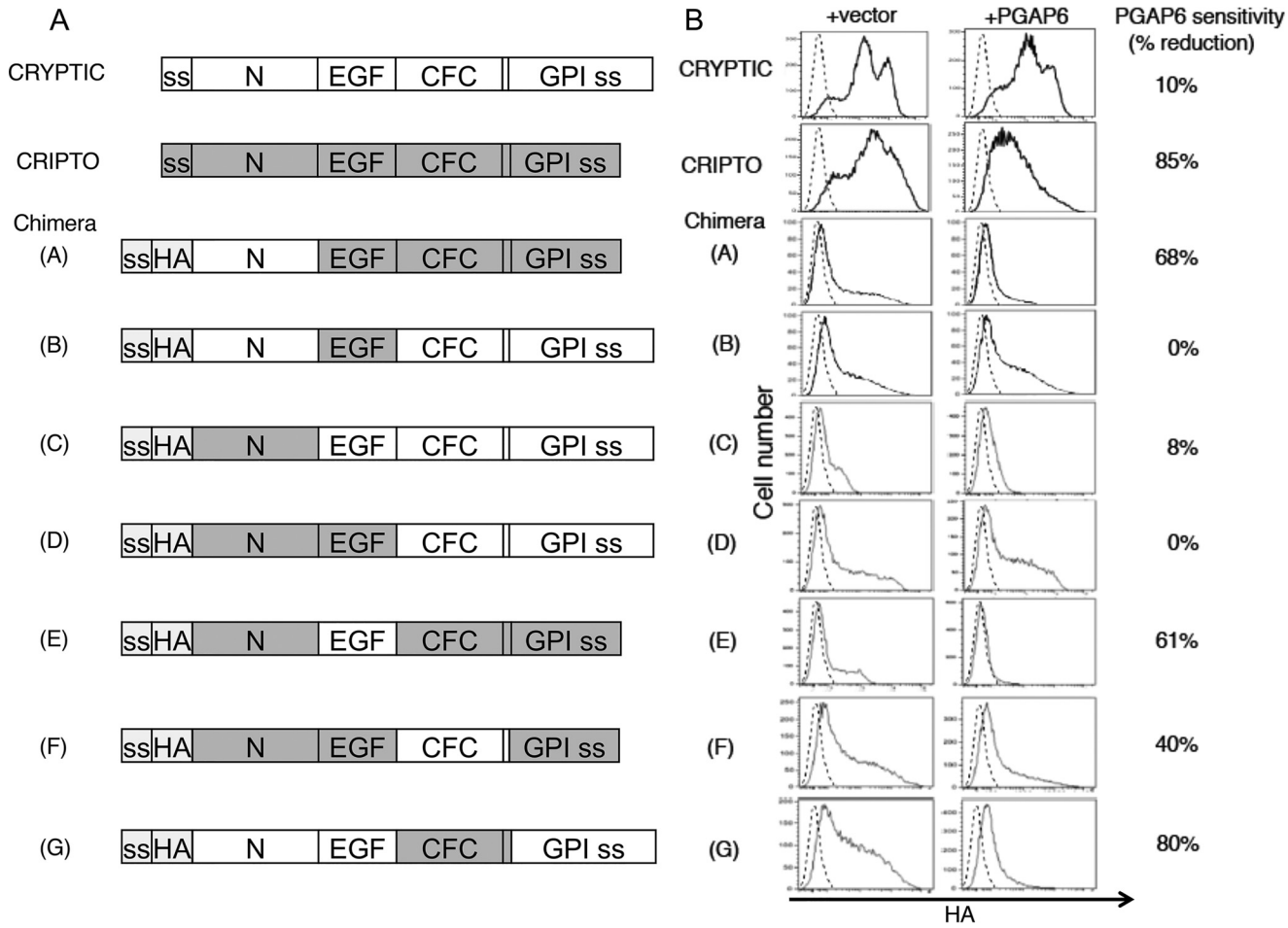

Figure 1. CFC domain of CRIPTO determines sensitivity to PGAP6. *A*, schematics of domain organizations of CRYPTIC, CRIPTO, and their seven domain-swapping chimeras (*panels A–G*). *ss*, signal sequence for ER localization; *EGF*, EGF-like domain; *CFC*, Cripto-1/FRL1/Cryptic domain; *GPI ss*, GPI attachment signal sequence. Short peptides of 6 and 10 amino acids in CRYPTIC and CRIPTO, respectively, connect CFC and GPI ss. *B*, cell-surface levels of CRYPTIC, CRIPTO, and their domain-swapping chimeras (*panels A–G*) on CHO cells with or without PGAP6 overexpression. PGAP6 sensitivity as determined by the percentage of reduction of expression levels with PGAP6 overexpression is indicated on the *right*. WT CRIPTO and CRYPTIC were tested under stable transfection, whereas chimeras were under transient transfection.

domain, an EGF-like domain, a CFC domain, and a GPI-attachment signal sequence (Fig. 1) (17). To understand the basis of the different sensitivities of CRIPTO and CRYPTIC to PGAP6 and to gain insight into the substrate recognition of PGAP6, we generated chimeric proteins between CRIPTO and CRYPTIC, in which corresponding domains were swapped, and their sensitivities to PGAP6 were tested. To achieve this, the chimeric cDNAs were transfected into Chinese hamster ovary (CHO) 3B2A cells with either an empty vector or PGAP6 cDNA, and the cell-surface levels of the chimeric proteins were determined by flow cytometry (Fig. 1). If a chimera is sensitive to PGAP6, one acyl-chain will be removed from the GPI anchor, and the lipid moiety becomes lyso-PI. The resulting chimeric protein with lyso-PI form of GPI anchor has only one acyl-chain for membrane association and will be quickly released from the cell surface like lyso-phospholipids (18, 19). Therefore, the cell-surface level of the chimera will be reduced by co-transfection with PGAP6. PGAP6 sensitivity was transferred to CRYPTIC by the introduction of the CRIPTO CFC domain into CRYPTIC (chimera G; Fig. 1*B*). However, introduction of the N and the EGF-like domains of CRIPTO into CRYPTIC did not confer sensitivity to PGAP6 (chimeras B, C, and D). Conversely, introduction of the CRYPTIC CFC domain into CRIPTO reduced the sensitivity of CRIPTO to PGAP6 (chimera F). Introduction of the N or the EGF-like domain of CRYPTIC into CRIPTO mildly affected sensitivity to PGAP6 (chimeras A and E). These results showed that the CFC domain confers sensitivity to PGAP6 and suggests that PGAP6 recognizes the CFC domain of CRIPTO for processing of its GPI anchor.

Site-directed CRIPTO mutants bearing amino acid substitutions in the CFC domain were generated to further analyze the basis of the CFC domain recognition by PGAP6 (Fig. 2). The CFC domains of both CRIPTO and CRYPTIC consist of ~50 amino acids including six conserved cysteines that make three disulfide bonds (Fig. 2*A*), suggesting that the CRIPTO and CRYPTIC CFC domains have a similar compact structure (20). Alanine mutations were introduced into residues of CRIPTO that are not conserved in CRYPTIC (*red* in Fig. 2*A*). Mutant CRIPTO proteins with mutations in the N-terminal region of the CFC domain were expressed at normal levels (m1, m2, and m4) or at mildly reduced levels (m3 and m5) (Fig. 2*B*) and displayed sensitivities to PGAP6 as WT CRIPTO (Fig. 2*C*). Mutant

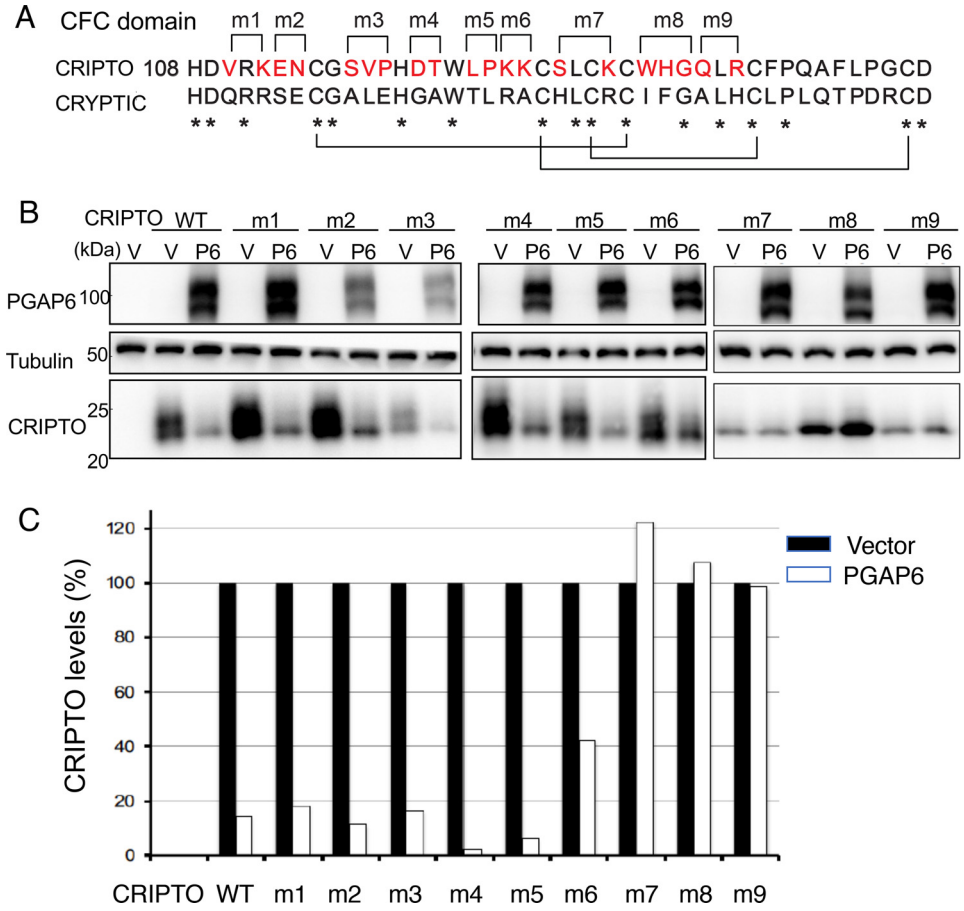

Figure 2. PGAP6 sensitivities of CRIPTO mutants bearing amino acid substitutions within the CFC domain. *A*, comparison of amino acid sequences of CFC domains of CRIPTO and CRYPTIC. *, conserved residues. *Red letters*, nonconserved residues substituted with alanines in mutants, m1–m9, indicated above. Three intradomain disulfide bonds are shown below sequences. *B*, levels of WT and mutant (m1–m9) CRIPTO proteins with vector (*V*) or PGAP6 (*P6*) co-transfection as assessed by Western blotting. *Top panels*, PGAP6; *middle panels*, tubulin; *bottom panels*, CRIPTO. *C*, levels of WT and mutant CRIPTO with PGAP6 co-transfection as assessed by flow cytometry. Levels of CRIPTO with vector co-transfection were taken as 100%.

CRIPTOs with mutations in the C-terminal region of the CFC (m7–m9) had reduced expression levels (Fig. 2*B*) and lost sensitivities to PGAP6 (Fig. 2*C*). The alanine mutations that reduced expression of the mutant CRIPTO might have affected efficiency of proper disulfide bond formation within the CFC domain. These results indicate that the C-terminal region of the CFC domain is critical for recognition by PGAP6.

The N-terminal region of PGAP6 is critical for recognition of CRIPTO

We next asked what part of PGAP6 is required for its activity against CRIPTO. PGAP6 consists of the signal sequence for ER translocation, a large N-terminal domain, an EGF domain, and seven TM domains (Fig. 3*A*). To determine the critical region for CRIPTO recognition, several truncation mutants of PGAP6 were generated and transfected into HEK293T cells expressing HA-tagged CRIPTO. The cell-associated and the released HA-tagged CRIPTO were assessed by Western blotting (Fig. 3*B*), and the cell-surface levels of HA-tagged CRIPTO were examined by flow cytometry (Fig. 3*C*). WT PGAP6 reduced the cell-surface levels of CRIPTO by 70% and increased the CRIPTO released into the culture medium. The N domain–deleted PGAP6 (ΔN) and the N domain and the EGF domain–deleted PGAP6 (ΔNEN) lost almost all activity, whereas the EGF domain–deleted PGAP6 (ΔEGF) had mildly reduced activity (Fig. 3), indicating that the N domain of PGAP6 is critical for activity.

PGAP6/TMEM8A, TMEM8B, and TMEM8C/myomaker share a common domain organization and form the TMEM8 protein family. Amino acids with putative catalytic involvement within the second and fifth TM domains are conserved in PGAP6/TMEM8A and TMEM8B. TMEM8C/myomaker is essential for myogenesis and hence termed myomaker (21). Some of the putative catalytic amino acids are not conserved in TMEM8C/myomaker, suggesting a nonenzymatic function. We generated a chimera consisting of the N and EGF domains of PGAP6 and the seven TM domains of TMEM8B (AnBc) to test whether TMEM8B has GPI-specific PLA2 activity (Fig. 3*A*). AnBc had CRIPTO-releasing activity comparable with PGAP6 (Fig. 3, *B* and *C*), supporting the concept that TMEM8B may also be a GPI-specific PLA2. To determine whether the N domain plus the EGF domain of TMEM8B have CRIPTO-recognizing function, another chimera consisting of the N and EGF domains of TMEM8B and the seven TM domains of PGAP6 was generated (BnAc). BnAc was inactive in CRIPTO

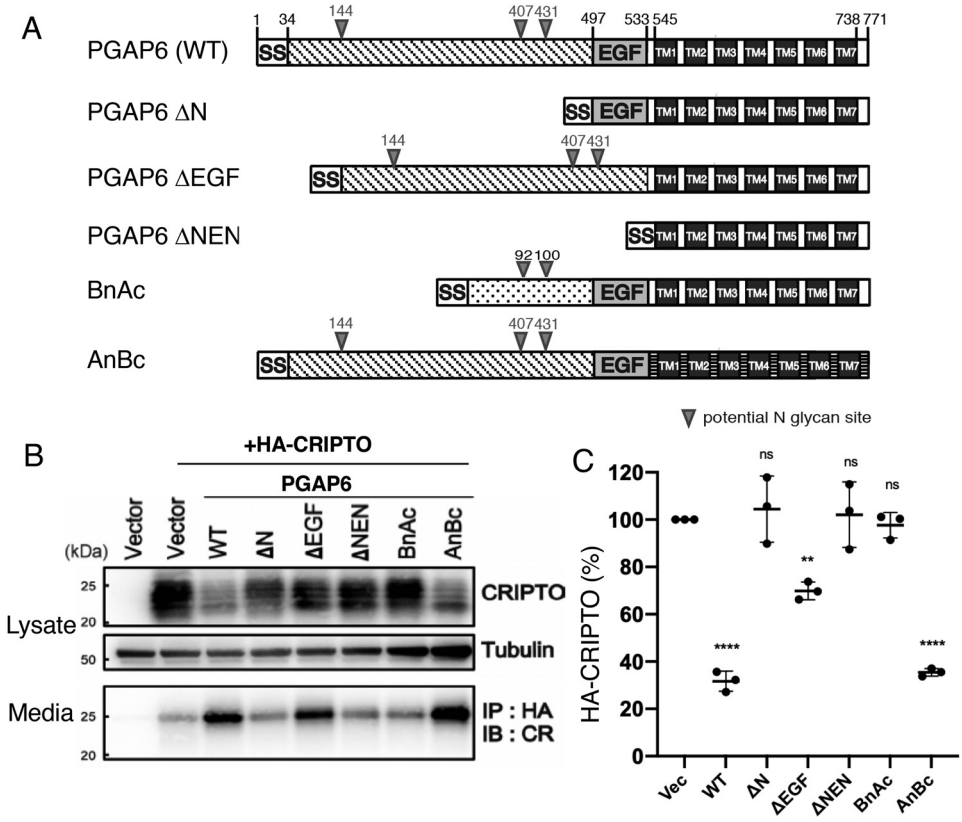

Figure 3. CRIPTO processing activities of truncation mutants of PGAP6 and chimeric proteins between PGAP6 and TMEM8B. *A*, schematic domain organizations of PGAP6 mutants and the chimeras. *B*, cells expressing HA-CRIPTO were transfected with WT PGAP6 or its truncation mutants lacking the N (Δ*N*), the EGF (Δ*EGF*), and the N plus the EGF (Δ*NEN*) domains, or chimeras of PGAP6 and TMEM8B. *BnAc*, N-terminal part of TMEM8B and C-terminal part of PGAP6; *AnBc*, N-terminal part of PGAP6 and C-terminal part of TMEM8B. Cell lysates and anti-HA immunoprecipitates from culture media were analyzed by Western blotting against anti-CRIPTO. Tubulin was used as a loading control. *C*, cell-surface levels of HA-CRIPTO after transfection of PGAP6, mutant PGAP6 and chimeras of PGAP6 and TMEM8B. Symbols of various PGAP6 constructs are the same as in *B*. Mean (*long horizontal bars*) and S.D. (*short horizontal bars*) of $n = 3$ are shown. *Vec*, vector; *IP*, immunoprecipitation; *IB*, immunoblot.

release (Fig. 3, *B* and *C*). The full-length TMEM8B was not stably expressed after transfection into several mammalian cell lines such as HEK293 and CHO, precluding further investigation of the substrate specificity of TMEM8B (data not shown).

To demonstrate physical interaction between PGAP6 and CRIPTO in the cells by a co-immunoprecipitation assay, an enzyme-dead mutant of PGAP6, D610A, was prepared by substituting the putative catalytic aspartic acid 610 with alanine. His-FLAG–tagged D610A PGAP6 (HF-PGAP6 D610A) was co-transfected with HA-tagged CRIPTO, CRYPTIC, or CD25 into HeLaS3 cells. Co-immunoprecipitation of HF-PGAP6 D610A with HA-tagged proteins was assessed by Western blotting against a rabbit anti-PGAP6 antibody. HF-PGAP6 D610A co-immunoprecipitated with HA-tagged CRIPTO but not with HA-tagged CRYPTIC and HA-tagged CD25 (Fig. 4), demonstrating that PGAP6 and CRIPTO specifically interact with each other in cells.

PGAP6 is not active toward a vast majority of GPI-APs, but GPC3, prostasin, SPACA4, and contactin-1 are sensitive to PGAP6

We next asked whether PGAP6 is active against other GPI-APs because the activity of PGAP6 involves specific recognition of a region of GPI-APs by the extracellular domain and the PGAP6 extracellular domain is large. To examine the specific recognition of PGAP6, the cDNAs of 79 human GPI-APs were cloned, and an HA tag was introduced at their N termini by replacing their ER translocation signal sequences with a CD59 signal sequence fused with HA. After transfection into HEK293 cells, the cell-surface expressions of 56 of 79 were confirmed by flow cytometry using an anti-HA antibody. PGAP6 sensitivity was assessed by percentage of reduction of the cell-surface levels of HA staining by co-overexpression of PGAP6. Of the 56 GPI-APs, only four other GPI-APs: GPC3, SPACA4 (sperm acrosome-associated protein 4, also known as SAMP14) (22), prostasin, and contactin-1, were sensitive to PGAP6, showing >60% reduction (Table 1 and Fig. 5*A* for SPACA4). Eight GPI-APs were mildly sensitive, showing 30% to 60% reduction by PGAP6 overexpression, whereas 43 other GPI-APs were either not sensitive or only slightly sensitive (Table 1). Therefore, PGAP6 has rather narrow specificity against GPI-APs.

We then examined sperm/testis expression of mouse and human PGAP6 because SPACA4/SAMP14 is expressed only in testis and sperm. PGAP6 was detected in lysates of mouse sperm and testis and human sperm by Western blotting using a rabbit polyclonal antibody raised against human PGAP6/

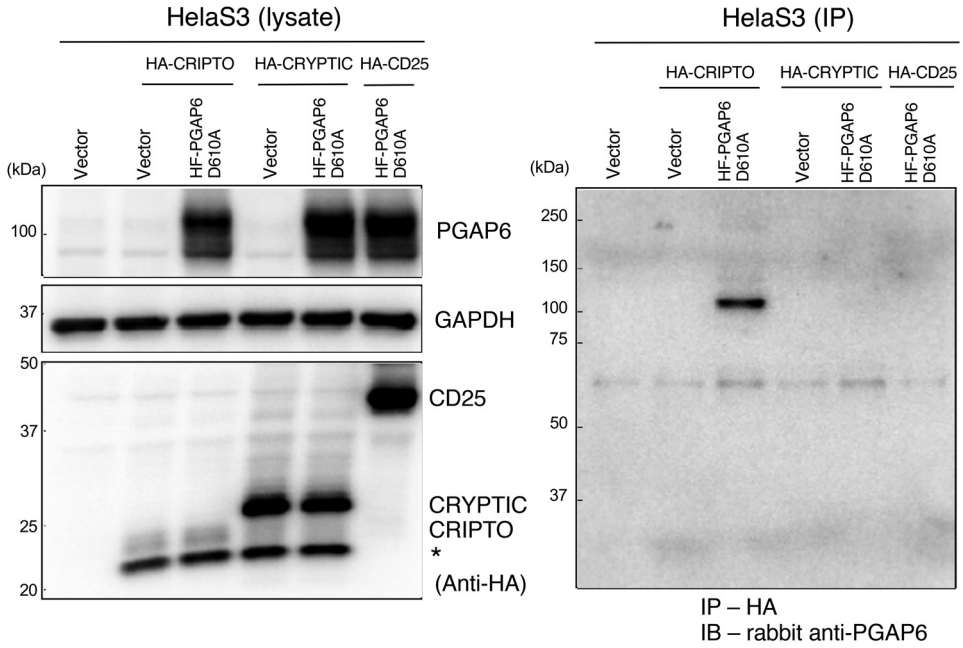

Figure 4. Physical association of PGAP6 and CRIPTO. An HF-tagged, enzyme dead PGAP6 mutant was co-transfected into HeLaS3 cells with HA-CRIPTO, HA-CRYPTIC, and HA-CD25 as a negative control. Anti-HA immunoprecipitates were analyzed by Western blotting against PGAP6 to determine co-precipitation (*right panel*). Expression levels of transfected proteins were assessed by Western blotting (*left panel*). GAPDH was used as a loading control. *, immature, ER forms of CRIPTO and CRYPTIC. *IP*, immunoprecipitation; *IB*, immunoblot.

TMEM8A (Fig. 5*B*). By immunofluorescence staining with the same antibody, PGAP6 was detected in the acrosomal cap (Fig. 5*C*). PGAP6 staining disappeared after the acrosomal reaction as indicated by widened IZUMO1 staining (Fig. 5*C*). Therefore, PGAP6 and SPACA4 are both expressed in the sperm head before the acrosomal reaction. However, whether PGAP6-dependent release of SPACA4 indeed occurs in sperm is yet to be determined. Two other sperm GPI-APs, LY6K and TEX101, which are substrates of another GPIase, tACE, were fully resistant to PGAP6 (Table 1). It was reported that SPACA4 is resistant to tACE (2, 3), further supporting that these GPIases are selective to certain GPI-APs.

Finally, the sensitivity of free, unlinked GPI to PGAP6 was examined. Some mouse tissues express free, unlinked GPI as free glycolipids (23). Cultured cell lines, defective in GPI-transamidase that attaches GPI to proteins, express high levels of free GPI on their surface (23). Transfection of PGAP6 into GPI-transamidase defective CHO cells reduced the level of free GPI by 88% as assessed by staining with the free GPI-specific T5 mAb (Fig. 6). These results suggest that PGAP6 accesses GPI when the protein part does not exist and that the protein parts of the vast majority of GPI-APs prohibit access of PGAP6 to the GPI moiety, whereas the protein parts of several GPI-APs allow PGAP6 access.

Discussion

Because of their glycolipid membrane anchors, GPI-APs can be potentially released from the cell surface by the actions of GPIases. Previously characterized GPIases are selective to only a few kinds of GPI-APs: GDE2 releases RECK and GPC6 (5,6), GDE3 releases uPAR and CNTFRα (7, 8), and tACE releases TEX101 and LY6K (2, 3). We reported previously that PGAP6 activity leads to the release of CRIPTO (9). Here, we report that PGAP6 is also active toward only a small number of GPI-APs. Among the 56 GPI-APs tested under PGAP6 overexpression conditions, only CRIPTO, GPC3, SPACA4, prostasin, and contactin-1 were highly sensitive to PGAP6. All of these previously characterized GPIase-mediated releases of select GPI-APs are the foundations of certain biological processes, such as neurogenesis, cell migration, sperm maturation and embryonic development. PGAP6-dependent release of GPC3, SPACA4, prostasin, and contactin-1 were shown only under PGAP6 overexpression conditions. Further studies are required to clarify whether the release of these proteins occurs under physiological conditions and to identify possible biological processes that are associated with the release of these proteins.

PGAP6 consists of a hydrophilic N-terminal extracellular part and a hydrophobic C-terminal part with seven TM domains. Our data showed that the extracellular part of PGAP6 recognizes the protein part of substrate GPI-APs. For CRIPTO, which has three distinct extracellular domains, the C-terminal region of the CFC domain is recognized by PGAP6. Because the extracellular part of PGAP6 is rather large (>500 amino acids), it may recognize other substrate GPI-APs. The hydrophobic C-terminal part of PGAP6 may form a catalytic region for the PI moiety in GPI. The second and the fifth TM domains contain putative catalytic amino acid residues conserved in TMEM8B and other CREST family members (11), such as PGAP3, a Golgi-resident GPI-APs-specific phospholipase A2 involved in fatty acid remodeling (24).

Table 1
Sensitivities of human GPI-APs to PGAP6

No.	GPI-AP	Gene name	Sensitivity[a]
1	CRIPTO	TDGF1	High
2	Glypican 3	GPC3	High
3	Sperm acrosome-associated protein 4	SPACA4	High
4	Prostasin	PRSS8	High
5	Contactin-1	CNTN1	High
6	Lymphocyte antigen 6D	LY6D	Medium
7	Ephrin A1	EFNA1	Medium
8	CD59	CD59	Medium
9	UL16-binding protein 1	ULBP1	Medium
10	Dipeptidase 2	DPEP2	Medium
11	CD55	CD55	Medium
12	CAMPATH-1 antigen	CD52	Medium
13	Ephrin A3	EFNA3	Medium
14	Ly6/PLAUR domain–containing protein 2	LYPD2	Low
15	Lymphocyte antigen 6E	LY6E	Low
16	Carboxypeptidase M	CPM	Low
17	Glial cell line–derived neurotrophic factor family receptor α-1	GFRA1	Low
18	Glypican 5	GPC5	Low
19	Ecto-ADP-ribosyltransferase 3	ART3	Low
20	Prion protein	PRNP	Resistant
21	Opioid-binding protein/cell adhesion molecule	OPCML	Resistant
22	Cilliary neurotrophic factor receptor subunit α	CNTFR	Resistant
23	Reversion-inducing cysteine-rich protein with Kazal motifs	RECK	Resistant
24	Alkaline phosphatase, non–tissue-specific isozyme	ALPL	Resistant
25	Alkaline phosphatase, germ cell type	ALPG	Resistant
26	Monocyte differentiation antigen CD14	CD14	Resistant
27	Signal transducer CD24	CD24	Resistant
28	CD48 antigen	CD48	Resistant
29	Carbonic anhydrase 4	CA4	Resistant
30	Carboxypeptidase O	CPO	Resistant
31	CRYPTIC	CFC1	Resistant
32	Ecto-ADP-ribosyltransferase 4	ART4	Resistant
33	Ectonucleotide pyrophosphatase family member 6	ENPP6	Resistant
34	Folate receptor α	FOLR1	Resistant
35	Glypican 1	GPC1	Resistant
36	Glypican 4	GPC4	Resistant
37	Lymphocyte antigen 6K	LY6K	Resistant
38	Lymphocyte antigen 6 complex G6C	LY6G6C	Resistant
39	Lymphocyte antigen 6 complex G6D	LY6G6D	Resistant
40	Ly6/PLAUR domain–containing protein 1	LYPD1	Resistant
41	Ly6/PLAUR domain–containing protein 6B	LYPD6B	Resistant
42	Netrin G1	NTNG1	Resistant
43	Neural cell adhesion molecule 1	NCAM1	Resistant
44	Neuronal growth regulator 1	NEGR1	Resistant
45	Neuritin	NRN1	Resistant
46	Neuritin-like protein	NRN1L	Resistant
47	Oligodendrocyte-myelin glycoprotein	OMG	Resistant
48	Pantetheinase	VNN1	Resistant
49	Prion-like Doppel	PRND	Resistant
50	Prostate stem cell antigen	PSCA	Resistant
51	Testis-expressed protein 101	TEX101	Resistant
52	Thy-1	THY1	Resistant
53	Tumor necrosis factor receptor superfamily 10C	TNFRSF10C	Resistant
54	UL16-binding protein 2	ULBP2	Resistant
55	Urokinase plasminogen activator surface receptor	PLAUR	Resistant
56	5′-Nucleotidase	NT5E	Resistant

[a] Percentage of reduction by PGAP6: high, >60%; medium, 30–60%; low, 10–30%; resistant, <10%.

We tested GPC1, GPC3, GPC4 and GPC5 for their sensitivities to overexpressed PGAP6. Only GPC3 was highly sensitive, whereas GPC5 was weakly sensitive, and GPC1 and GPC4 were essentially insensitive. GPC5 may not be sensitive to PGAP6 under physiological expression levels of PGAP6. GPC6 is reported to be sensitive to GDE2. Therefore, at least two GPCs, GPC3 and GPC6, are sensitive to GPI-cleaving/processing phospholipases.

Experimental procedures

Antibodies, cells, and materials

T5_4E10 mAb (T5 mAb) against free GPI-GalNAc (mouse IgM) was kindly provided by Dr. Jean François Dubremetz (Montpellier University, Montpellier, France) (25). T5_4E10 mAb is available from BEI Resources, ATCC (catalog No. NR-50267). Mouse anti-human PGAP6/TMEM8A mAb (clone 5C3, IgG2b) was a gift from Bio Legend Japan (Osaka, Japan). Polyclonal rabbit anti-PGAP6 was raised by immunization with a peptide corresponding to the C-terminal cytosolic tail of mouse PGAP6 (Scrum). Monoclonal rabbit anti-CRIPTO was from Cell Signaling Technology. Rat anti-mouse IZUMO1 mAb (clone KS64-125) was reported previously (2, 26). mAb anti-GAPDH (clone 6c5, Thermo Fisher), anti–HA tag (H7), anti-acetylated tubulin (clone 6-11B-1) (Sigma–Aldrich), and anti-tubulin and anti-transferrin receptors (Zymed Laboratories Inc., South San Francisco, CA, USA) were purchased. Secondary antibodies used were horseradish peroxidase

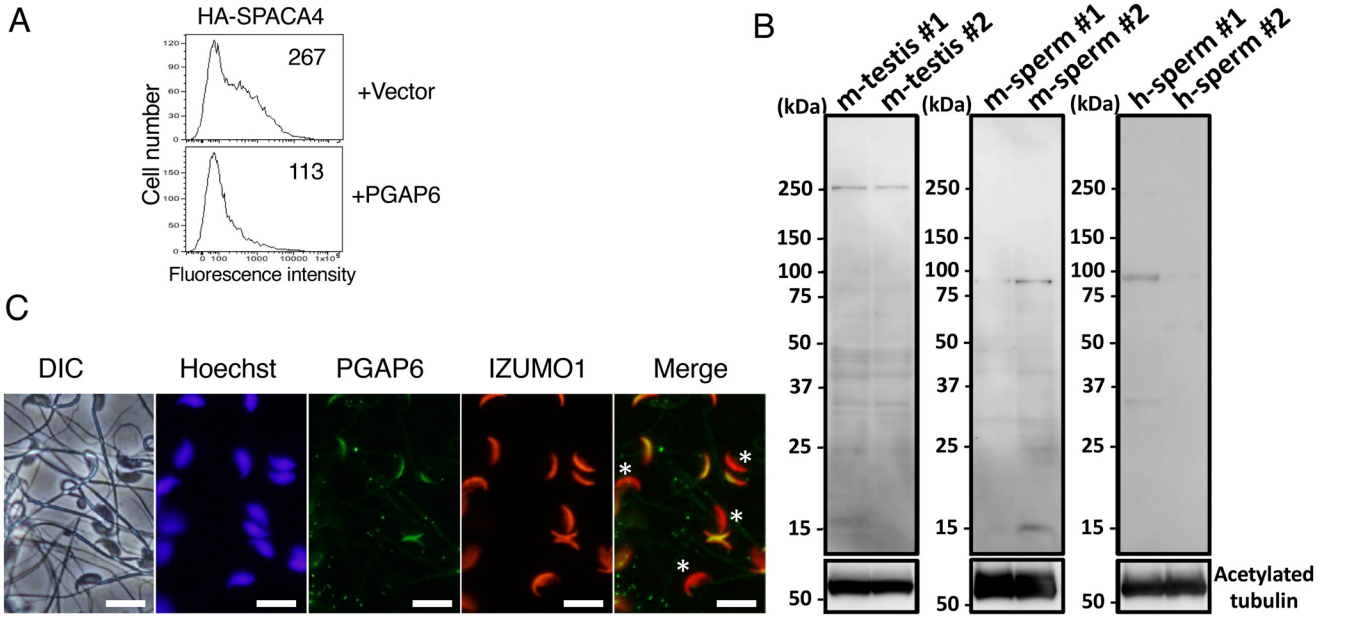

Figure 5. PGAP6 sensitivity of SPACA4 and expression of PGAP6 in testis and sperm. *A*, sensitivity of SPACA4 to PGAP6. HEK293 cells expressing HA-SPACA4 were co-transfected with vector (*top panel*) or PGAP6 (*bottom panel*). Mean fluorescence intensities of anti-HA staining are shown in the panels. Background fluorescence intensity was 36. *B*, Western blotting determination of PGAP6 in mouse testis and mouse and human sperm. The testis PGAP6 appeared twice as big as the sperm PGAP6. *C*, immunofluorescence staining of mouse sperm for PGAP6. PGAP6 was present in the acrosomal cap and disappeared after the acrosomal reaction. *, acrosome reacted sperm indicated by wider IZUMO1 staining. *Scale bars*, 10 μm. *DIC*, differential interference contrast.

(HRP)–conjugated anti-mouse IgG (GE Healthcare) and anti-rabbit IgG (Cell Signaling Technology), phycoerythrin-conjugated goat anti-mouse IgG (BD Biosciences and PharMingen, San Diego, CA), Alexa 488–conjugated goat anti-mouse IgM, Alexa 488–conjugated goat anti-mouse IgG and goat anti-rabbit IgG, and Alexa 594–conjugated goat anti-rabbit IgG (Life Technologies).

HEK293T cells stably expressing HA-tagged CRIPTO were established by transfection of linearized pME-pgkpuro-HA-CR1 and cultured in Dulbecco's modified Eagle's medium containing 10% fetal calf serum and 10 μg/ml puromycin as described before (9). To prepare pME-pgkpuro-HA-CR1, we obtained human CRIPTO cDNA (Kazusa DNA Research Institute, Kisarazu, Japan) and cloned it into a mammalian expression plasmid pME bearing puromycin resistance gene and a segment of signal sequence plus HA tag. CHO cells used in this study were CHO 3B2A cells derived from CHO-K1 cells (ATCC) and stably express two human GPI-APs: CD59 and DAF (27). All CHO cell lines including WT 3B2A and 3B2A cells stably expressing HA-PGAP6, His-FLAG-PGAP6, PGAP6-FLAG, or HA-CRYPTIC (human CRYPTIC HA-tagged at the N terminus after the ER signal sequence) were cultured in Ham's F-12 medium containing 10% fetal calf serum with 6 μg/ml blasticidin, 10 μg/ml puromycin, or 500 μg/ml hygromycin, if necessary. Human CRYPTIC cDNA (clone AK315326) was obtained from NITE Biological Resource Center (Kisarazu, Japan). HeLa S3 cells (ATCC) were stably transfected with HA-CRIPTO, HA-CRYPTIC, and HA-CD25. They were then transiently transfected with an empty pME or pME bearing His-FLAG–tagged PGAP6 with D610A mutation (HF-PGAP6 D610A).

Plasmids of human GPI-APs' cDNAs were obtained from Invitrogen. Their protein coding regions lacking the N-terminal signal sequences were cloned into pME expression vector bearing an N-terminal signal sequence of CD59 plus HA tag so that N-terminally HA-tagged GPI-APs are expressed.

Mouse and human samples

Mouse testis and sperm were obtained from 10-week-old B6D2F1 mice. Animal experiments were approved by the Animal Care and Use Committee of the Research Institute for Microbial Diseases, Osaka University, Japan. Human sperm were obtained from a volunteer after consent. Experiments using human samples were approved by the Ethics Committee of the Research Institute for Microbial Diseases, Osaka University, Osaka, Japan, and abide by the Declaration of Helsinki principles. Lysates of sperm and testis were prepared in a lysis buffer (6 M urea, 2 M thiourea, and 2% sodium deoxycholate). PGAP6 and acetylated tubulin as a loading control were detected by Western blotting against rabbit polyclonal antibody to human PGAP6 and anti-tubulin antibody. PGAP6 and IZUMO1 in mouse sperm were detected by immunofluorescence staining by rabbit polyclonal antibody to human PGAP6 (1 in 50 dilution) and rat mAb to mouse IZUMO1 (1 in 500 dilution) after incubation of sperm in TYH medium (28) for 2 h.

Flow cytometry

The cells were incubated with mouse T5 mAb (1 in 1,000 dilution of ascites) or anti-HA in FACS buffer (PBS containing

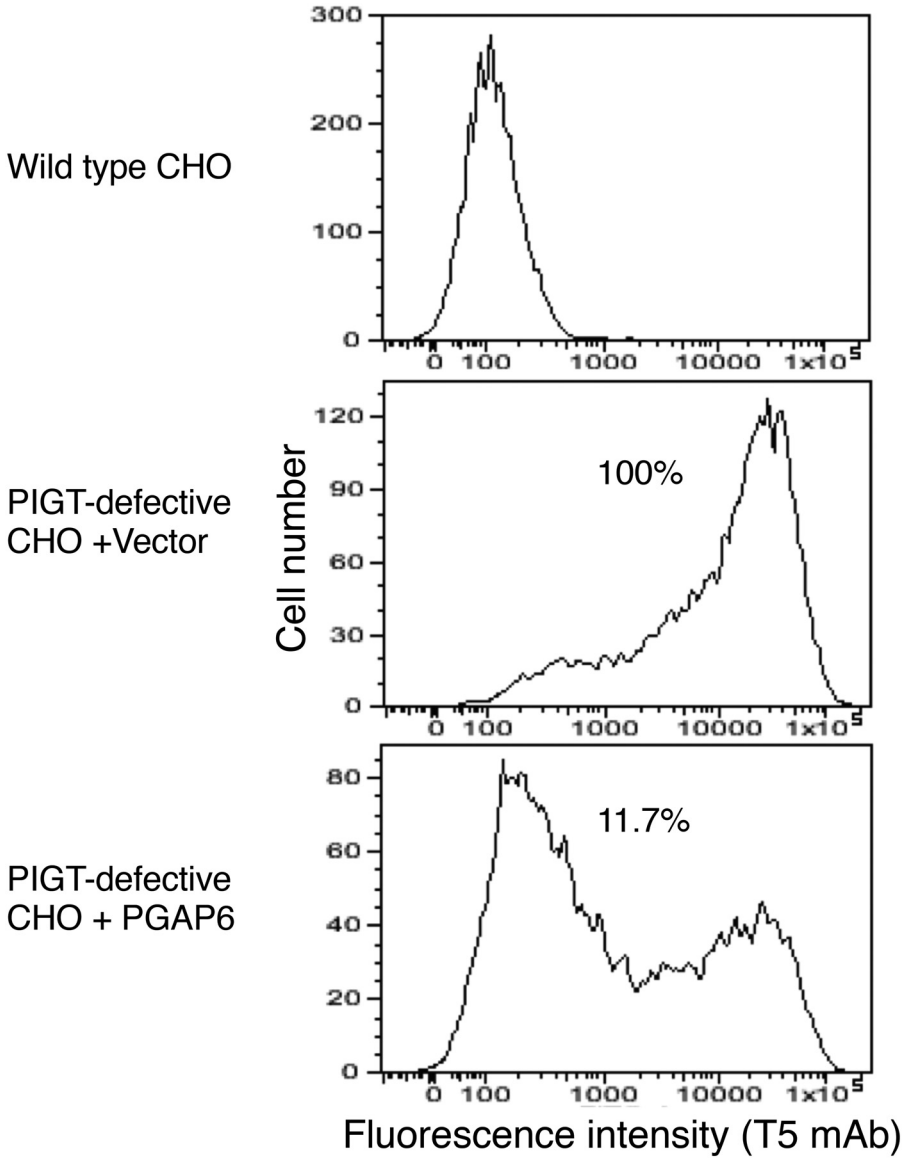

Figure 6. Sensitivity of free, unlinked GPI to PGAP6. WT CHO3B2A (*top panel*) and PIGT-defective CHO cells transfected with vector (*middle panel*) or PGAP6 (*bottom*) were stained by T5 mAb that recognizes free GPI bearing GalNAc side chain. Mean fluorescence intensity on the PGAP6-transfected cells was 11.7% of that on the vector-transfected cells.

1% BSA and 0.1% NaN_3) on ice for 25 min. The cells were then washed twice in FACS buffer followed by staining with Alexa Fluor 488–conjugated goat anti-mouse IgM for T5 mAb and phycoerythrin-conjugated goat anti-mouse IgG for anti-HA in FACS buffer. After washing twice with FACS buffer, the cells were analyzed by the BD FACSCanto II.

Western blotting

The samples were run on 10–20% gradient SDS-PAGE gels followed by transfer to polyvinylidene difluoride membranes. The polyvinylidene difluoride membranes were blocked with 5% nonfat milk in TBS/Tween 20 at room temperature for 1 h. PGAP6, HA-tagged proteins, tubulin, and GAPDH were detected using rabbit anti-PGAP6, and mouse anti-HA, anti-tubulin and anti-GAPDH (1:4000) followed by detection with HRP-conjugated anti-rabbit IgG and HRP-conjugated anti-mouse IgG (1:4000).

Data availability

All data from this study are contained within the article and may be shared upon request to the corresponding author.

Acknowledgments—We thank Dr. Jean-François Dubremetz (Montpellier University) for T5 4E10 mAb and the Edanz Group (RRID: SCR_014013) for editing a draft of this article.

Author contributions—G.-H. L. data curation; G.-H. L. and H. M. investigation; G.-H. L., M. F., H. N., H. M., M. I., Y. Maeda, and Y. Murakami writing-review and editing; M. F. and T. K. conceptualization; M. F. and T. K. supervision; M. F. and T. K. funding

acquisition; H. N. and M. I. resources; Y. Maeda and Y. Murakami methodology; T. K. writing-original draft; T. K. project administration.

Funding and additional information—This work was supported by Japan Society for Promotion of Science (JSPS) and Ministry of Education, Culture, Sports, Science and Technology (MEXT) KAKENHI Grants JP16H04753 and 17H06422 (to T. K.) and a grant for Joint Research Project of the Research Institute for Microbial Diseases, Osaka University (to M. F. and T. K.).

Conflict of interest—The authors declare that they have no conflicts of interest with the contents of this article.

Abbreviations—The abbreviations used are: GPI, glycosylphosphatidylinositol; CFC, Cripto-1/FRL1/Cryptic; GPI-AP, GPI-anchored protein; GPIase, GPI-specific hydrolytic enzymes; tACE, testis-specific angiotensin-converting enzyme; GDE, glycerophosphodiesterase; GPC, glypican; PLA2, phospholipase A_2; TM, transmembrane; EGF, epidermal growth factor; ER, endoplasmic reticulum; CHO, Chinese hamster ovary; N domain, N-terminal domain; HA, hemagglutinin; HRP, horseradish peroxidase; GAPDH, glyceraldehyde-3-phosphate dehydrogenase.

References

1. Kinoshita, T. (2020) Biosynthesis and biology of mammalian GPI-anchored proteins. *Open Biol.* **10,** 190290 CrossRef Medline
2. Fujihara, Y., Tokuhiro, K., Muro, Y., Kondoh, G., Araki, Y., Ikawa, M., and Okabe, M. (2013) Expression of TEX101, regulated by ACE, is essential for the production of fertile mouse spermatozoa. *Proc. Natl. Acad. Sci. U.S.A.* **110,** 8111–8116 CrossRef Medline
3. Fujihara, Y., Okabe, M., and Ikawa, M. (2014) GPI-anchored protein complex, LY6K/TEX101, is required for sperm migration into the oviduct and male fertility in mice. *Biol. Reprod.* **90,** 60 CrossRef Medline
4. Kondoh, G., Tojo, H., Nakatani, Y., Komazawa, N., Murata, C., Yamagata, K., Maeda, Y., Kinoshita, T., Okabe, M., Taguchi, R., and Takeda, J. (2005) Angiotensin-converting enzyme is a GPI-anchored protein releasing factor crucial for fertilization. *Nat. Med.* **11,** 160–166 CrossRef Medline
5. Park, S., Lee, C., Sabharwal, P., Zhang, M., Meyers, C. L., and Sockanathan, S. (2013) GDE2 promotes neurogenesis by glycosylphosphatidylinositol-anchor cleavage of RECK. *Science* **339,** 324–328 CrossRef Medline
6. Matas-Rico, E., van Veen, M., Leyton-Puig, D., van den Berg, J., Koster, J., Kedziora, K. M., Molenaar, B., Weerts, M. J., de Rink, I., Medema, R. H., Giepmans, B. N., Perrakis, A., Jalink, K., Versteeg, R., and Moolenaar, W. H. (2016) Glycerophosphodiesterase GDE2 promotes neuroblastoma differentiation through glypican release and is a marker of clinical outcome. *Cancer Cell* **30,** 548–562 CrossRef Medline
7. van Veen, M., Matas-Rico, E., van de Wetering, K., Leyton-Puig, D., Kedziora, K. M., De Lorenzi, V., Stijf-Bultsma, Y., van den Broek, B., Jalink, K., Sidenius, N., Perrakis, A., and Moolenaar, W. H. (2017) Negative regulation of urokinase receptor activity by a GPI-specific phospholipase C in breast cancer cells. *eLife* **6,** e23649 CrossRef Medline
8. Dobrowolski, M., Cave, C., Levy-Myers, R., Lee, C., Park, S., Choi, B. R., Xiao, B., Yang, W., and Sockanathan, S. (2020) GDE3 regulates oligodendrocyte precursor proliferation via release of soluble CNTFRα. *Development* **147,** dev180695 CrossRef Medline
9. Lee, G. H., Fujita, M., Takaoka, K., Murakami, Y., Fujihara, Y., Kanzawa, N., Murakami, K. I., Kajikawa, E., Takada, Y., Saito, K., Ikawa, M., Hamada, H., Maeda, Y., and Kinoshita, T. (2016) A GPI processing phospholipase A2, PGAP6, modulates Nodal signaling in embryos by shedding CRIPTO. *J. Cell Biol.* **215,** 705–718 CrossRef Medline
10. Fagerberg, L., Hallström, B. M., Oksvold, P., Kampf, C., Djureinovic, D., Odeberg, J., Habuka, M., Tahmasebpoor, S., Danielsson, A., Edlund, K., Asplund, A., Sjöstedt, E., Lundberg, E., Szigyarto, C. A., Skogs, M., *et al.* (2014) Analysis of the human tissue-specific expression by genome-wide integration of transcriptomics and antibody-based proteomics. *Mol. Cell. Proteomics* **13,** 397–406 CrossRef Medline
11. Pei, J., Millay, D. P., Olson, E. N., and Grishin, N. V. (2011) CREST: a large and diverse superfamily of putative transmembrane hydrolases. *Biol. Direct* **6,** 37 CrossRef Medline
12. Minchiotti, G., Parisi, S., Liguori, G., Signore, M., Lania, G., Adamson, E. D., Lago, C. T., and Persico, M. G. (2000) Membrane-anchorage of Cripto protein by glycosylphosphatidylinositol and its distribution during early mouse development. *Mech. Dev.* **90,** 133–142 CrossRef Medline
13. Tian, T., and Meng, A. M. (2006) Nodal signals pattern vertebrate embryos. *Cell. Mol. Life Sci.* **63,** 672–685 CrossRef Medline
14. Shen, M. M. (2007) Nodal signaling: developmental roles and regulation. *Development* **134,** 1023–1034 CrossRef Medline
15. Ding, J., Yang, L., Yan, Y. T., Chen, A., Desai, N., Wynshaw-Boris, A., and Shen, M. M. (1998) Cripto is required for correct orientation of the anterior–posterior axis in the mouse embryo. *Nature* **395,** 702–707 CrossRef Medline
16. Chu, J., and Shen, M. M. (2010) Functional redundancy of EGF-CFC genes in epiblast and extraembryonic patterning during early mouse embryogenesis. *Dev. Biol.* **342,** 63–73 CrossRef Medline
17. Shen, M. M., and Schier, A. F. (2000) The EGF-CFC gene family in vertebrate development. *Trends Genet.* **16,** 303–309 CrossRef Medline
18. Holthuis, J. C., and Levine, T. P. (2005) Lipid traffic: floppy drives and a superhighway. *Nat. Rev. Mol. Cell Biol.* **6,** 209–220 CrossRef Medline
19. Lev, S. (2010) Non-vesicular lipid transport by lipid-transfer proteins and beyond. *Nat. Rev. Mol. Cell Biol.* **11,** 739–750 CrossRef Medline
20. Foley, S. F., van Vlijmen, H. W., Boynton, R. E., Adkins, H. B., Cheung, A. E., Singh, J., Sanicola, M., Young, C. N., and Wen, D. (2003) The CRIPTO/FRL-1/CRYPTIC (CFC) domain of human Cripto: functional and structural insights through disulfide structure analysis. *Eur. J. Biochem.* **270,** 3610–3618 CrossRef Medline
21. Millay, D. P., O'Rourke, J. R., Sutherland, L. B., Bezprozvannaya, S., Shelton, J. M., Bassel-Duby, R., and Olson, E. N. (2013) Myomaker is a membrane activator of myoblast fusion and muscle formation. *Nature* **499,** 301–305 CrossRef Medline
22. Shetty, J., Wolkowicz, M. J., Digilio, L. C., Klotz, K. L., Jayes, F. L., Diekman, A. B., Westbrook, V. A., Farris, E. M., Hao, Z., Coonrod, S. A., Flickinger, C. J., and Herr, J. C. (2003) SAMP14, a novel, acrosomal membrane-associated, glycosylphosphatidylinositol-anchored member of the Ly-6/urokinase-type plasminogen activator receptor superfamily with a role in sperm–egg interaction. *J. Biol. Chem.* **278,** 30506–30515 CrossRef Medline
23. Wang, Y., Hirata, T., Maeda, Y., Murakami, Y., Fujita, M., and Kinoshita, T. (2019) Free, unlinked glycosylphosphatidylinositols on mammalian cell surfaces revisited. *J. Biol. Chem.* **294,** 5038–5049 CrossRef Medline
24. Maeda, Y., Tashima, Y., Houjou, T., Fujita, M., Yoko-O, T., Jigami, Y., Taguchi, R., and Kinoshita, T. (2007) Fatty acid remodeling of GPI-anchored proteins is required for their raft association. *Mol. Biol. Cell* **18,** 1497–1506 CrossRef Medline
25. Tomavo, S., Couvreur, G., Leriche, M. A., Sadak, A., Achbarou, A., Fortier, B., and Dubremetz, J. F. (1994) Immunolocalization and characterization of the low molecular weight antigen (4–5 kDa) of *Toxoplasma gondii* that elicits an early IgM response upon primary infection. *Parasitology* **108,** 139–145 CrossRef Medline
26. Ikawa, M., Tokuhiro, K., Yamaguchi, R., Benham, A. M., Tamura, T., Wada, I., Satouh, Y., Inoue, N., and Okabe, M. (2011) Calsperin is a testis-specific chaperone required for sperm fertility. *J. Biol. Chem.* **286,** 5639–5646 CrossRef Medline
27. Nakamura, N., Inoue, N., Watanabe, R., Takahashi, M., Takeda, J., Stevens, V. L., and Kinoshita, T. (1997) Expression cloning of PIG-L, a candidate *N*-acetylglucosaminyl-phosphatidylinositol deacetylase. *J. Biol. Chem.* **272,** 15834–15840 CrossRef Medline
28. Muro, Y., Hasuwa, H., Isotani, A., Miyata, H., Yamagata, K., Ikawa, M., Yanagimachi, R., and Okabe, M. (2016) Behavior of mouse spermatozoa in the female reproductive tract from soon after mating to the beginning of fertilization. *Biol. Reprod.* **94,** 80 CrossRef Medline